11474 *J. Phys. Chem. A* **1999,** *103,* 11474−11480

Matrix Isolation and Density Functional Study of the Reaction of $OVCl_3$ with CH_3OH: Synthesis and Characterization of $Cl_2V(O)OCH_3$

Bruce S. Ault*

Department of Chemistry, University of Cincinnati, P.O. Box 210172, Cincinnati, Ohio 45221

Received: September 16, 1999; In Final Form: November 2, 1999

The matrix isolation technique has been employed to investigate the reaction of $OVCl_3$ with CH_3OH. Using twin jet deposition, the initial intermediate in the mechanism was identified as a weakly bound molecular complex. This species is characterized by perturbations to the C−O, V═O, and V−Cl stretching modes. Merged jet deposition, with a room-temperature reaction zone, led to complete conversion to $Cl_2V(O)OCH_3$, the second intermediate in the reaction sequence, through HCl elimination from the initial complex. This species was identified by use of extensive isotopic labeling, the observation of HCl as an additional reaction product, and by comparison to density functional calculations. All of the fundamental vibrational modes of this species that lie above 400 cm^{-1} were observed, some with very high intensities. Heating the reaction zone above 150 °C led to destruction of this intermediate, and production of both CH_2O and CH_3Cl.

Introduction

High valent transition metal oxo compounds form a class of very strong oxidizing agents toward a wide range of organic substrates. Vanadium oxytrichloride, Cl_3VO, is a prototypical member of this group, vigorously oxidizing many organic reagents.[1,2] However, very little is known experimentally concerning the mechanism of these reactions, including the identity of key intermediates. On the other hand, a series of theoretical studies have been carried out in recent years, with the aim of providing a better understanding of the mechanisms, intermediates, and energetics in reactions of transition metal oxo compounds.[3−7]

The matrix isolation technique[8−10] was developed to facilitate the isolation and characterization of reactive intermediates. The approach has been applied to the study of a wide range of species, including radicals, ions, and weakly bound molecular complexes. A recent matrix isolation study[11] explored the reaction between $CrCl_2O_2$ and CH_3OH and was able to identify three distinct steps in the mechanism and to characterize the intermediates in each step. The use of different deposition techniques for matrix formation, each with its own time scale, permitted the observation of sequential intermediates in this study. While there are clearly similarities between $CrCl_2O_2$ and $OVCl_3$, there are certain differences in the chemistry of Cr(VI) and V(V) compounds. Thus, a study was undertaken to examine the reaction of $OVCl_3$ with CH_3OH followed by trapping to argon matrices.

Experimental Section

All of the experiments in this study were conducted on conventional matrix isolation apparatus that has been described.[12] In the flowing gas reactor, referred to as merged jet deposition,[13] the two gaseous reactants, each diluted in argon, were prepared in separate gas-handling manifolds. The two deposition lines were then joined with an Ultratorr tee at a distance from the cryogenic surface, and the flowing gas samples were permitted to mix and react during passage through the merged region which was constructed of 316 stainless steel. The length of this region was variable, from 4 to 100 cm. In addition, the merged region could be heated to as high as 300 °C, to induce further reaction. The flowing gas mixture exited the tip of the deposition line and was sprayed onto the 14 K cold surface for 20−24 h before final infrared spectra were recorded on a Nicolet IR42 Fourier transform infrared spectrometer at 1 cm^{-1} resolution. Additional experiments were conducted in the twin jet mode, where the two reactants, each diluted in argon, were co-deposited on the cold surface from separate nozzles. A number of these matrices were subsequently warmed to 33−35 K to permit annealing and limited diffusion and then recooled to 14 K and additional spectra recorded.

Oxyvanadium trichloride (Aldrich) was introduced into the vacuum system as the vapor above the room-temperature liquid, after purification in a glass finger by freeze−pump−thaw cycles. The room temperature vapor pressure of OVCl3, approximately 10 mmHg, was sufficient for the preparation of premixed gaseous samples. The vacuum manifold containing the $OVCl_3$ sample needed extensive conditioning with $OVCl_3$ vapor before good samples could be prepared. CH_3OH (Aldrich), CD_3OH, CD_3OD, $^{13}CH_3OH$, and $CH_3{}^{18}OH$ (all Cambridge Isotope Laboratories, 99% isotopic enrichment) were also introduced as the vapor above the room-temperature liquid, after repeated freeze−pump−thaw cycles. Argon was used as the matrix gas in all experiments and was used without further purification.

Theoretical calculations were conducted on the likely intermediate species in this study, using the Gaussian 94 suite of programs.[14] Both restricted Hartree−Fock and density functional calculations employing the Becke functional B3LYP were conducted to locate stable minima, determine structures, and calculate vibrational spectra. Final calculations with full geometry optimization employed the 6-311G* triple-ζ basis set, after initial calculations with smaller basis sets were run to approximately locate energy minima. Calculations were carried out on a Silicon Graphics Indigo 2 workstation.

Results

Blank experiments of each reagent in solid argon were conducted for each of the reagents in this study, prior to any

10.1021/jp993318q CCC: $18.00

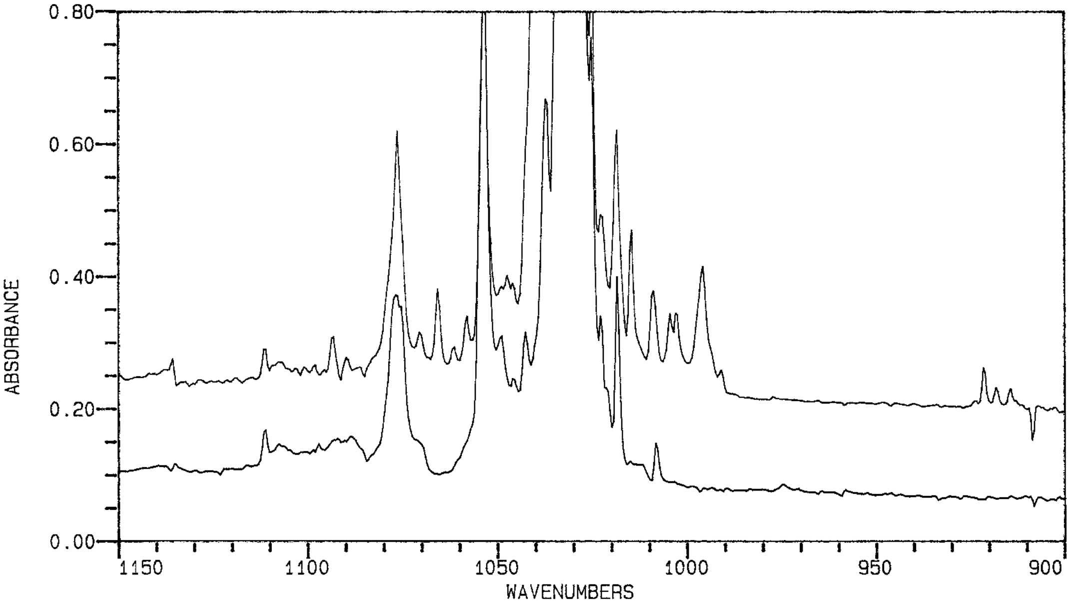

Figure 1. Infrared spectrum of a matrix prepared by the twin jet co-deposition of a sample of Ar/CH_3OH = 250 with a sample of Ar/$OVCl_3$ = 500 (top trace) compared to the spectrum of a matrix prepared by the deposition of a sample of Ar/CH_3OH = 250 with additional argon (lower trace). The bands marked with an asterisk are due to the 1:1 complex.

co-deposition experiments. The spectra obtained in these blanks were in good agreement with literature spectra;[15,16] traces of HCl (0.01−0.05 absorbance units) were noted[17] in all Ar/$OVCl_3$ experiments, and some CD_3OH was noted in the CD_3OD blank experiments.. These blank experiments were then annealed to approximately 35 K and recooled to 14 K and additional spectra recorded. Some aggregation was noted for the CH_3OH samples, while no change was noted for annealed matrices containing $OVCl_3$.

Twin Jet Experiments. In an initial experiment, a sample of Ar/CH_3OH = 250 was co-deposited with a sample of Ar/$OVCl_3$ = 500 using twin jet deposition. Four weak new absorptions were noted in the resulting spectrum, as 440, 996, 1092, and 2525 cm^{-1}; the region from 900 to 1150 cm^{-1} is shown in Figure 1. Intense bands due to the parent species were noted as well. This matrix was then annealed to 35 K and recooled to 14 K, at which point an additional spectrum was recorded. All four of the above bands grew as a result of annealing, by approximately 25%. Several additional twin jet experiments were then conducted, using different sample concentrations, with variations from 250/1 to 1000/1 for each reagent. In all of these experiments, the four bands listed above were observed. Three, at 440, 996, and 1092 cm^{-1}, maintained a constant intensity ratio with respect to one another (within the uncertainty in the intensity measurements) and will hereafter be referred to as set A, while the last band at 2525 cm^{-1} did not maintain a constant intensity ratio with respect to the other three bands. Annealing these matrices led to an increase in band intensity in each case.

Twin jet experiments were also conducted in which samples of Ar/$OVCl_3$ were co-deposited with samples of Ar/$^{13}CH_3OH$, Ar/CD_3OD, and Ar/$CH_3{}^{18}OH$ in different experiments. For each system, similar results were obtained. The bands near 440 and 2525 cm^{-1} were observed in each case, unshifted relative to the normal isotopic species. The band observed at 996 cm^{-1} for the normal isotopic species shifted to 978 cm^{-1} upon ^{13}C substitution, to 970 cm^{-1} upon ^{18}O substitution, and to 951 cm^{-1} upon deuteration. The band near 1092 cm^{-1} for the normal isotopic species was difficult to detect, due to overlap with parent bands for certain of the isotopic species. This band did not appear to shift with ^{13}C substitution, while the region was obscured with ^{18}O substitution, and only appeared as a shoulder on an intense parent band when fully deuterated methanol was employed. When each of these matrices were annealed to 35 K and recooled, the product bands all grew somewhat in intensity. The band at 2525 cm^{-1} again did not maintain a constant intensity ratio with respect to the other bands in this series of experiments.

Merged Jet Experiments. When a sample of Ar/CH_3OH = 500 was co-deposited with a sample of Ar/$OVCl_3$ = 500 in a merged jet experiment with a 90 cm reaction zone held at room temperature, *the results were dramatically different from those obtained in the twin jet experiments.* Bands due to the parent reagents were completely absent from the spectrum, as were the product bands observed in the twin jet experiments, and a series of intense new bands were observed. These were located at 446, 502, 674, 1030, 1069, 1121, 1152, 1430, 1444, 1447, 1725, 1733, 1746, 2827, 2933, and 2940 cm^{-1}. Some of these bands (e.g., those at 502, 1030, and 1069 cm^{-1}) had intensities greater than 1.0 absorbance units, as shown in Figure 2. In addition, bands at 2863 and 2888 cm^{-1} due to HCl (always present in trace amounts in $OCVl_3$ experiments) grew very substantially in these merged jet experiments. Additional merged jet experiments were carried out with these two reagents and a room-temperature reaction zone, varying the respective concentrations of the Ar/CH_3OH and Ar/$OVCl_3$ samples over a wide range. In experiments where CH_3OH was in excess, the above product bands were observed along with parent bands of CH_3OH, but with lower intensities than in CH_3OH blank experiments. Likewise, when $OVCl_3$ was in excess, these product bands were observed, along with weaker bands due to $OVCl_3$. In all of these experiments, the level of HCl was greatly increased relative to Ar/$OVCl_3$ blank experiments. The product bands at 446, 502, 674, 1030, 1069, 1121, 1152, 1430, 1444, 1447, 2827, 2933, and 2940 cm^{-1} all maintained a constant intensity ratio with respect to one another over this series of merged jet experiments and will be hereafter referred to as set B. The bands at 1725, 1733, and 1746 cm^{-1} did not maintain a constant intensity ratio with respect to the bands in set B and will be referred to as set C.

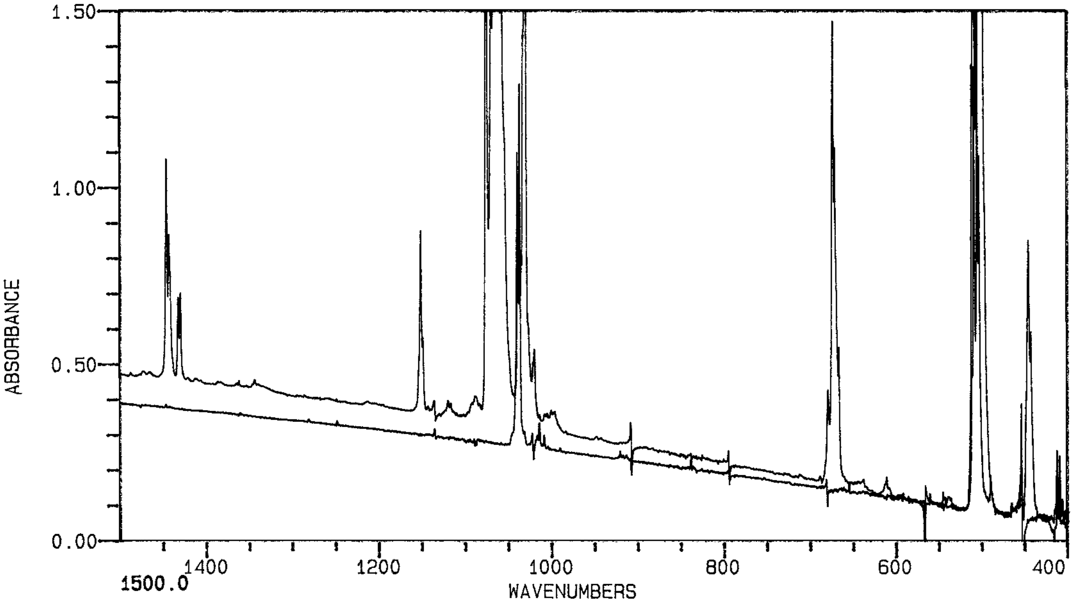

Figure 2. Infrared spectrum of a matrix prepared by the room-temperature merged jet co-deposition of a sample of Ar/CH_3OH = 500 with a sample of Ar/$OVCl_3$ = 500 (top trace) compared to the infrared spectrum of a matrix prepared by the deposition of a sample of Ar/$OVCl_3$ = 500 with additional argon (lower trace).

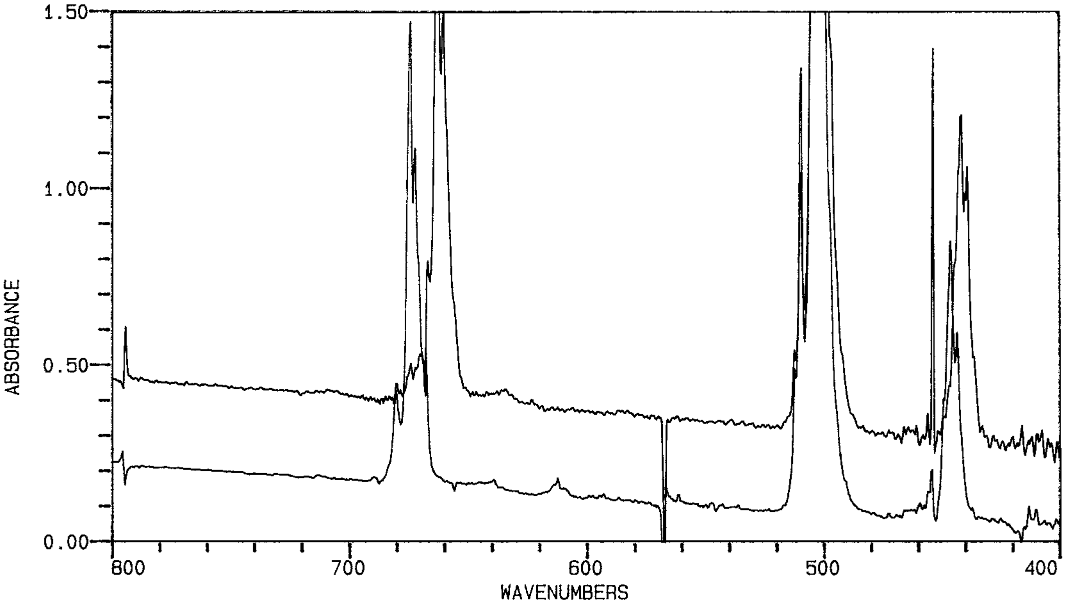

Figure 3. Infrared spectrum of a matrix prepared by the room-temperature merged jet deposition of a sample of Ar/$CH_3{}^{18}OH$ = 500 with a sample of Ar/$OVCl_3$ = 500 (upper trace) compared to the infrared spectrum of a matrix prepared by the merged jet co-deposition of a sample of Ar/CH_3-16OH = 500 with a sample of Ar/$OVCl_3$ = 500 (lower trace).

Additional merged jet experiments were conducted by varying the length of the merged region, while maintaining the region at room temperature. When the length of the region was reduced to 20 cm, very similar results were observed. The same product bands were seen with high intensity, and there was almost complete loss of the parent bands. However, when the reaction zone was shortened further, so that the two lines joined only 4 cm from the cold window, then the above set of product bands was observed with greatly diminished intensity. At the same time, bands due to the parent species were observed with substantial intensity, although still reduced relative to comparable blank experiments.

Some 90 cm merged jet experiments were also conducted in which samples of Ar/$OVCl_3$ were co-deposited with samples of Ar/$^{13}CH_3OH$, Ar/$CH_3{}^{18}OH$, and Ar/CD_3OD in separate sets of experiments. Throughout these experiments, very similar results were obtained; representative spectra are shown in Figure 3. An extensive set of product bands was observed, with a dramatic reduction or complete loss of bands due to the parent reagents. Some of the product bands were observed to shift relative to experiments with the normal isotope, while other product bands were unshifted in these experiments. When CD_3OD was employed, the two most intense bands of DCl were observed.[17] Table 2 lists all of the product bands for species B observed in these isotopic labeling experiments.

Pyrolysis Experiments. A number of experiments were conducted in the merged jet mode, with the reaction zone heated above room temperature. When a sample of Ar/CH_3OH = 250 was copyrolyzed to 150 °C in this manner with a sample of Ar/$OVCl_3$ = 500, *all of the intense product bands observed in the room temperature merged jet experiments were completely absent*. Instead, a series of weak-to-medium bands grew in, at

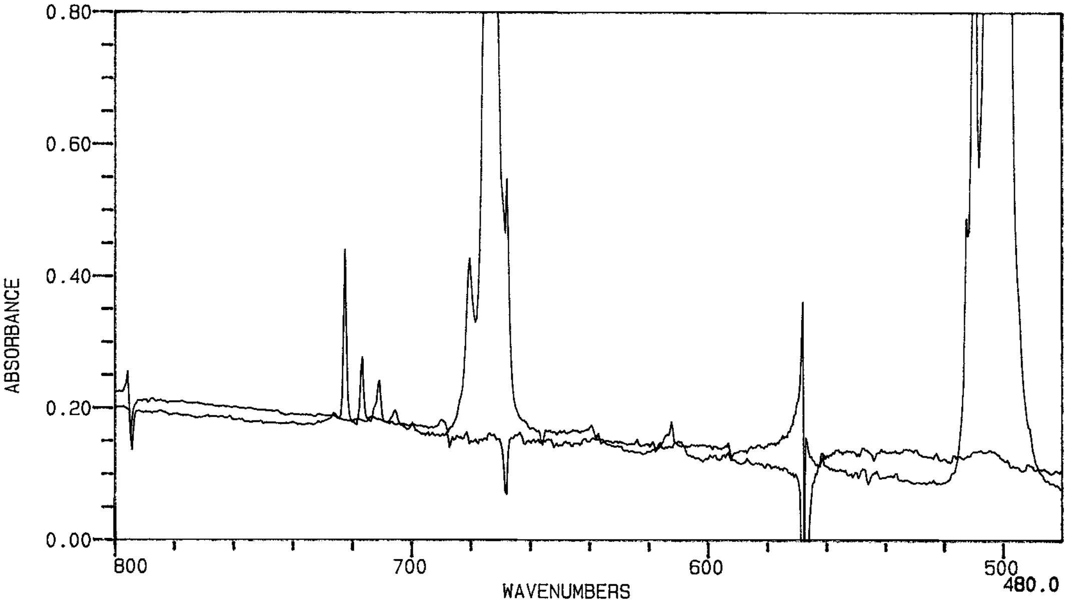

Figure 4. Infrared spectrum of a matrix prepared by the merged jet co-deposition with pyrolysis to 160 °C of a sample of $Ar/CH_3OH = 500$ with a sample of $Ar/OVCl_3 = 500$ compared to the infrared spectrum of a similar matrix prepared by room-temperature merged jet co-deposition (i.e., without pyrolysis).

TABLE 1: Band Positions (cm^{-1}) and Assignments for the 1:1 Complex of $OVCl_3$ with CH_3OH

$OVCl_3{\cdot}CH_3OH$	$OVCl_3{\cdot}CH_3{}^{18}OH$	$OVCl_3{\cdot}{}^{13}CH_3OH$	$OVCl_3{\cdot}CD_3OD$	parent band[a]	assignment
440	440	440	440	502	V−Cl stretch
996	970	978	951	1031	C−O stretch
1092	1092	1092	1097	1042	V=O stretch

[a] For the normal isotopic species.

710, 718, 721, 1350, 1445, 1499, 1727, 1742, 2964, and 3040 cm^{-1}; Figure 4 shows the spectrum in the low-energy region for such a sample, compared to an unpyrolyzed merged jet experiment. In addition, growth in the bands due to HCl was noted compared to a similar room-temperature merged jet experiment. Similar experiments were conducted at a variety of pyrolysis temperatures. When the temperature of the reaction zone was less than 140−150 °C, no reaction was observed. When the temperature was above 150 °C, then complete reaction took place. The bands at 710, 718, 721, 1350, 1445, 1499, 2964, and 3040 cm^{-1} maintained a constant intensity ratio with respect to one another and will be referred to as set D. The remaining bands, at 1500, 1727, and 1742 cm^{-1}, will be referred to as set E. Pyrolysis experiments were also conducted with isotopically labeled CH_3OH; comparable product bands were noted, some of which showed small shifts relative to the normal isotope, and others showed no shift.

Discussion

Numerous product bands and several product species were isolated in the reaction of $OVCl_3$ with CH_3OH under a range of reaction conditions. As noted above, many of the product bands can be grouped into sets, based on the conditions under which they appeared and the fact that bands within a given set maintained a constant intensity ratio with respect to other bands in that set. It is also apparent that the different product species are formed in sequence, as reaction conditions are altered, the time available for reaction increased, and additional energy deposited into the system. The identity of the species responsible for each set of product bands will be discussed, followed by the results of ab initio calculations and an overview of the mechanism of reaction.

Product Identification

The bands in set A were formed under the conditions of shortest reaction time and lowest reaction temperature, namely in the twin jet deposition experiments where mixing of the two reactants occurs on the surface of the condensing matrix. This indicates the species A is the initial intermediate in the reaction between $OVCl_3$ and CH_3OH. Further, while the yield of species A was quite low during deposition, bands due to species A grew upon annealing the matrix to 33 K. Thus, the barrier to formation of A from the isolated reactants must be very low. This is indicative of the formation of a molecular complex between the two subunits.[18] Spectroscopically, this would be manifested by a shifting of certain vibrational modes of the two subunits, particularly modes involving atoms at the site of complexation. Since CH_3OH is known to serve as a proton donor in hydrogen bonding interactions and $OVCl_3$ has four very electronegative ligands, hydrogen bond formation is reasonable. Alternatively, coordination through the oxygen of CH_3OH to the highly positive vanadium center on $OVCl_3$ is possible. Spectroscopically, the vibrational mode of the CH_3OH subunit most perturbed by the formation of the complex was the C−O stretch, as shown in Table 1. The isotopic shifts of this bands with ^{13}C, ^{18}O, and $-CD_3$ substitution were very similar to the shifts of the same mode for parent CH_3OH. The 1092 cm^{-1} product band is tentatively assigned as the perturbed V=O stretch in the complex, shifted to higher energy, while the 440 cm^{-1} is assigned to a perturbed V−Cl stretching mode. All of these observations point to the identification of species A as a complex between CH_3OH and $OVCl_3$, the initial intermediate for this pair of reactants. The low number and intensity of the bands due to this complex precludes a definitive determination of the structure of the complex. Finally, in the twin jet experiments a

TABLE 2: Band Positions (cm^{-1}) and Assignments for Argon Matrix Isolated $Cl_2V(O)OCH_3$

$Cl_2V(O)OCH_3$	$Cl_2V(O)^{18}OCH_3$	$Cl_2V(O)O^{13}CH_3$	$Cl_2V(O)OCD_3$	assignment
446	442	446	443	VCl_2 stretch
502	502	502	502	VCl_2 stretch
674	662	666	646	V−O stretch
1030	1028	1030	1030	V═O stretch
1069[a]	1039[a]	1056[a]	1066[a]	C−O stretch
1121		1114	887	CH_3 rock
1152	1148	1144	897	CH_3 rock
1430	1421	1427	1085	CH_3 def
1444	1443	1442	1050	CH_3 asym def
1447	1445	1444	1050	CH_3 asym def
2827	2826	2826	2050	CH_3 sym. st
2933	2932	2928	2179	CH_3 asym st
2940	2940	2935	2186	CH_3 asym st

[a] Center of multiplet.

band was observed at 2525 cm^{-1} that could not be attributed to this molecular complex. Rather, this band matches[23] the H−Cl stretching mode of the HCl complex with CH_3OH. Since residual HCl is present in all experiments employing $OVCl_3$, and since CH_3OH is present as well, formation of this complex is anticipated.

Merged jet reaction, which provides a longer reaction time and a reaction zone at room temperature, led to complete reaction between $OVCl_3$ and CH_3OH, with no remaining reactant or initial complex. Instead, set B was observed, as described above. Many of these bands were very intense, indicative of complete conversion to product. Importantly, the amount of HCl present in the merged jet experiments was significantly greater than in the twin jet experiments, indicating that HCl is produced in the merged jet experiments. Moreover, merged jet experiments between $OVCl_3$ and CD_3OD led to DCl formation, while twin jet experiments between these two reagents showed traces of amount of HCl (residual in the $OVCl_3$ sample), and no DCl. This demonstrates that the merged jet reaction between $OVCl_3$ and CH_3OH generates HCl (DCl) as one of the products.

The intermediate species remaining after HCl elimination from the molecular complex would be $Cl_2V(O)OCH_3$, a species that is a methoxy derivative of parent $OVCl_3$. Chemical intuition suggests that such a species should be stable. Also, as will be discussed below, DFT calculations predict that $Cl_2V(O)OCH_3$ to be stable, and the calculated spectrum agrees very well with the observed bands of set B, including isotopic shifts. In the analogous reactions[11,19] of $CrCl_2O_2$ and $TiCl_4$ with CH_3OH, similar HCl elimination reactions were observed, leading in each case to a methoxy derivative of the parent compound. *Thus, species B is identified as the HCl elimination product of the initial complex, $Cl_2V(O)OCH_3$.* As will be discussed below, this conclusion is not fully consistent with the calculations of Ziegler[3] which suggest that the addition/hydrogen shift product, $Cl_3V(OH)OCH_3$, is the second intermediate in the reaction pathway. Band positions and assignments for $Cl_2V(O)OCH_3$ are collected in Table 2.

The species responsible for the set C bands was also produced in minor amounts in these merged jet experiments. Set C bands, at 1725, 1733, and 1746 cm^{-1}, lie within 2 cm^{-1} of bands due to matrix isolated[20] CH_2O and the HCl complex[21] of CH_2O. In addition, the shift of these bands upon isotopic substitution matched the shift reported in the literature.[20,21] The HCl stretching mode of the $HCl{\cdot}CH_2O$ complex region has been observed near 2628 cm^{-1}. However, the very low yield of the complex in the present study precluded observation of this feature. CH_2O is the direct oxidation product of CH_3OH and was also observed in the reaction between $CrCl_2O_2$ and CH_3OH, albeit at higher temperatures. Thus, the set C bands are assigned to CH_2O and to the $CH_2O{\cdot}HCl$ complex, formed as a very minor secondary product in the room-temperature merged jet experiments. The small shift in band positions relative to previous study suggests that the CH_2O formed in this manner is perturbed just slightly, although there is not sufficient information to identify the perturbing species.

TABLE 3: Calculated (B3LYP/G-311G*) Structural Parameters for $Cl_2V(O)OCH_3$

parameter	calculated value
R(V═O)	1.5539 Å
R(V−Cl)	2.1686 Å
R(V−O)	1.7185 Å
R(O−C)	1.4199 Å
R(C−H)[a]	1.092 Å
α(O═V−Cl)	108.8°
α(Cl−V−O)	109.9°
α(V−O−C)	135.7°
α(O−C−H)[b]	109.1°
α(H−C−H)[c]	109.9°

[a] Average value (range from 1.0920 to 1.0928 Å). [b] Average value (range from 108.4° to 110.4°). [c] Average value (range from 109.6° to 110.1°).

Experiments were also run in which the reaction zone was heated above 150 °C. In these experiments, bands due to $Cl_2V(O)OCH_3$ were completely destroyed, demonstrating that this species has a limited range of thermal stability. When this species was destroyed, new bands were noted in the spectrum, in addition to continued growth of HCl. These new bands, sets D and E, are readily assigned by comparison to authentic spectra. Set D bands are assigned[22] to CH_3Cl and the HCl complex[23] of CH_3Cl. This species was observed as the thermal decomposition product of Cl_3TiOCH_3, and the present study demonstrates that it is also formed in the thermal decomposition of $Cl_2V(O)OCH_3$. The set E bands match exactly the most intense fundamentals[20] of CH_2O and the HCl complex[21] of CH_2O. These are very close to the set C bands above and represent CH_2O without the slight perturbation that is present in the room temperature merged jet experiments. The overall yield of CH_2O is greater in the pyrolysis experiments than in the experiments with a room temperature reaction zone. It is clear that additional products containing vanadium must form in these experiments as well. These do not survive to the depositing matrix, and are likely deposited on the walls of the merged jet reaction region.

Theoretical Calculations

The two most likely products in the merged jet reaction are the addition/hydrogen transfer product $Cl_3V(OH)OCH_3$ and the HCl elimination product $Cl_2V(O)OCH_3$. Density functional

TABLE 4: Calculated (B3LYP 6-311G*) and Observed Frequencies above 400 cm^{-1} and Isotopic Shifts for $Cl_2V(O)OCH_3$

normal isotope		^{18}O		^{13}C		CD_3		
calcd freq[a]	exptl freq	calcd shift	exptl shift	calcd shift	exptl shift	calcd shift	exptl shift	description
456 (443)	446	−5	−4	0	0	−4	−3	VCl_2 stretch
506 (491)	502	0	0	0	0	0	0	VCl_2 stretch
692 (674)	674	−12	−12	−7	−8	−32	−28	V−O stretch
1104 (1072)	1069	−36	−30	−15	−13	1	−3	C−O stretch
1134 (1101)	1030	−1	−2	−1	0	10	0	V═O stretch
1168 (1134)	1121	−4		−8	−7	−265	−234	CH_3 rock
1182 (1148)	1152	−6	−4	−8	−8	−268	−255	CH_3 rock
1481 (1438)	1430	−3	−2	−5	−2	−379	−345	CH_3 sym deformation
1498 (1455)	1444	0	−1	−2	−3	−418	−394	CH_3 asym deformation
1499 (1456)	1447	0	−1	−2	−3	−418	−397	CH_3 asym deformation
3032 (2925)	2827	−1	−4	−3	−4	−864	−777	CH_3 sym stretch
3115 (3025)	2933	0	−1	−12	−5	−802	−754	CH_3 asym stretch
3118 (3028)	2940	0	0	−12	−5	−801	−754	CH_3 asym stretch

[a] Listed bands are unscaled; bands in parentheses are scaled by a factor of 0.97.

calculations were carried out for these two species, using the B3LYP functional and the 6-311G* basis set. Both species optimized to stable energy minima; the structure found for $Cl_3V(OH)OCH_3$ was quite similar to that found by Ziegler. The calculated structure of $Cl_2V(O)OCH_3$ is given in Table 3. Vibrational frequencies were then calculated at the energy minimum for both species, using the same method and basis set. In both cases, all positive frequencies were found. Vibrational frequencies were also calculated for the ^{13}C, ^{18}O, and $-CD_3$ isotopically labeled species, also for comparison to the experimental spectra. Table 4 lists the calculated frequencies above 400 cm^{-1} for the normal isotopic species and compares these to the experimental frequencies. Also listed are the calculated and experimental isotopic shifts for all of vibrational modes. For example, the V−O stretching mode is calculated at 692 cm^{-1} (unscaled) and observed at 674 cm^{-1} [using the standard scaling factor[24] for B3LYP/6-311G* of 0.9739, the calculated band position is 674 cm^{-1}, identical to the experimental band position]. The calculated isotopic shifts are −8, −9, and −27 cm^{-1} for ^{18}O, ^{13}C, and $-CD_3$, while the experimental values are −12, −8, and −28 cm^{-1}, respectively. The only difficulties arise in the 1000−1100 cm^{-1} region, where two fundamentals are calculated for the normal isotope and some mode mixing occurs. However, based on isotopic shifts, the product bands can be assigned, and the experimental shifts agree very well with the calculated values. For $Cl_2V(O)OCD_3$, the three $-CD_3$ bending modes shift into the 1000−1100 cm^{-1} region, leaving five fundamentals within a small wavenumber range. For this species, individual band assignments in this region must be regarded as somewhat tentative. Nonetheless, the overall match between the experimental and the theoretical spectrum is excellent.

The agreement between the experimental spectrum and the spectrum calculated for the potential hydrogen transfer product, $Cl_3V(OH)OCH_3$, is very poor in many areas. For example, the calculations indicate that only one band should be observed in the 1000−1100 cm^{-1} region, the C−O stretch, while two intense bands were seen. The calculated spectrum predicted a band of moderate intensity between 800 and 850 cm^{-1}, while the experimental spectrum showed nothing in this region. The calculated spectrum also predicted the most intense band in the spectrum to be at 699 cm^{-1}, due to the V−O−H bending mode. This band was predicted to have isotopic shifts of 0, 0, and −1 cm^{-1} for ^{13}C, ^{18}O, and $-CD_3$ substitution, respectively. Experimentally, the only band near this position was at 674 cm^{-1}. This band was only moderately intense and had isotopic shifts of −7, −12, and −28 cm^{-1} for ^{13}C, ^{18}O, and $-CD_3$ substitution. The V−O stretch was calculated to be at 614 cm^{-1}, while it was actually observed at 676 cm^{-1}. Last, the experimental spectrum had an extremely intense band at 502 cm^{-1} assigned to the VCl_2 antisymmetric stretching mode. The calculated spectrum for $Cl_3V(OH)OCH_3$ predicts all of the V−Cl stretching modes to be near 400 cm^{-1}, with no bands predicted near 500 cm^{-1}. Thus, comparison of the calculated spectrum to the experimental spectrum, combined with the observation of HCl as a reaction product in the merged jet reaction, demonstrates that $Cl_3V(OH)OCH_3$ is not responsible for the new infrared absorptions and provides further support for the identification of $Cl_2V(O)OCH_3$ as the absorbing species.

Mechanistic Inferences

A series of intermediates have been suggested over the years to explain the role of $OVCl_3$ in the oxidation of CH_3OH and other organic substrates. The calculations of Ziegler and co-workers[3] suggest that this reaction occurs by hydrogen transfer from CH_3OH to the oxo group of $OVCl_3$ to form the intermediate $Cl_3V(OH)OCH_3$. In their parallel study[4] of the oxidation of CH_3OH by $CrCl_2O_2$, they proposed an analogous process and intermediate. In the latter system, they considered the possibility of HCl elimination and formation of a methoxy derivative of the parent compound but then ruled out this pathway. Experimental work has now demonstrated that the reaction *does* follow the HCl elimination pathway and that the intermediate methoxy derivative does decompose at high temperatures to CH_2O. In the former ($OVCl_3$) case, they did not report any calculations on the HCl elimination pathway, but rather they focused only on the hydrogen addition pathway. The experimental work reported here demonstrates that, *under the conditions employed here*, the HCl elimination pathway is dominant, leading to $Cl_2V(O)OCH_3$ in essentially 100% yield. It should be noted that the conditions employed here, a flow reactor with stainless steel walls, might allow for wall or surface reactions instead of, or in addition to, gas-phase reaction. In the earlier $CrCl_2O_2/CH_3OH$ study, the wall material of the reaction zone was varied and no change was noted in product formation. Nonetheless, the possibility of wall reactions cannot be eliminated.

Two stable products were observed during the pyrolysis of $Cl_2V(O)OCH_3$, namely, CH_2O and CH_3Cl. The former is the expected oxidation product, while the latter represents a reaction channel not leading to oxidation. In the analogous reaction of CH_3OH with $CrCl_2O_2$, only CH_2O formation was observed, while in the reaction of CH_3OH with $TiCl_4$, only CH_3Cl was seen. Apparently, the energetics of decomposition of $Cl_2V(O)OCH_3$ are such that both channels are allowed.

However, since the absolute absorption coefficients of CH_2O and CH_3Cl in argon matrices are not known, the branching ratio between these two channels cannot be determined.

Conclusions

Twin jet and merged jet matrix isolation experiments led to the formation of a series of intermediate products in the oxidation of CH_3OH by $OVCl_3$. Initially formed was a 1:1 complex, a species that further reacted at room temperature to eliminate HCl and produce $Cl_2V(O)OCH_3$. Pyrolysis above 150 °C of $Cl_2V(O)OCH_3$ in a flowing gas reactor followed by matrix trapping led to destruction of this species and the production of CH_2O and CH_3Cl, along with additional HCl.

Acknowledgment. The National Science Foundation is gratefully acknowledged for their support of this research through Grant CHE98-77076.

References and Notes

(1) Crans, D. C.; Chen, H.; Felty, R. A. *J. Am. Chem. Soc*. **1992**, *114*, 4543.

(2) Yajima, A.; Matsuzaki, R.; Saeki, Y. *Bull Chem. Soc. Jpn*. **1978**, *51*, 1098.

(3) Deng, L.; Ziegler, T. *Organometallics* **1996**, *15*, 3011.

(4) Deng, L.; Ziegler, T. *Organometallics* **1997**, *16*, 716.

(5) Ziegler, T.; Li, J. *Organometallics* **1995**, *14*, 214.

(6) Rappe, A. K.; Goddard, W. A., III *Nature* **1980**, *285*, 311.

(7) Rappe, A. K.; Goddard, W. A., III, *J. Am. Chem. Soc*. **1982**, *104*, 3287.

(8) Craddock, S.; Hinchliffe, A. *Matrix Isolation*; Cambridge University Press: Cambridge, 1975.

(9) Hallam, H. E. *Vibrational Spectroscopy of Trapped Species*; John Wiley: New York, 1973.

(10) Andrews, L., Moskovitz, M. Eds. *Chemistry and Physics of Matrix Isolated Species*; Elsevier Science Publishers: Amsterdam, 1989.

(11) Ault, B. S. *J. Am. Chem. Soc*. **1998**, *120*, 6105.

(12) Ault, B. S. *J. Am. Chem. Soc*. **1978**, *100*, 2426.

(13) Carpenter, J. D.; Ault, B. S. *J. Phys. Chem.* **1991**, *95*, 3502.

(14) Frisch, M. J.; Trucks, G. W.; Schlegel, H. B.; Gill, P. M. W.; Johnson, B. G.; Robb, M. A.; Cheeseman, J. R.; Keith, T.; Petersson, G. A.; Montgomery, J. A.; Raghavachari, K.; Al-Laham, M. A.; Zakrzewski, V. G.; Ortiz, J. V.; Foresman, J. B.; Cioslowski, J.; Stefanov, B. B.; Nanayakkara, M.; Challacombe, M.; Peng, C. Y.; Ayala, P. Y.; Chen, W.; Wong, M. W.; Andres, J. L.; Binkley, J. S.; Defrees, D. J.; Baker, J.; Stewart, J. P.; Head-Gordon, M.; Gonzalez, C.; Pople, J. A. *Gaussian 94*, revision E.1; Gaussian, Inc.: Pittsburgh, PA, 1995.

(15) Filgueira, R. R.; Fournier, L. L.; Varetti, E. L. *Spectrochim. Acta* **1982**, *38A*, 965.

(16) Barnes, A. J.; Hallam, H. E. *Trans. Faraday Soc*. **1970**, *66*, 1920.

(17) Maillard, D.; Schriver, A.; Perchard, J. P.; Girardet, C. *J. Chem. Phys*. **1979**, *71*, 505.

(18) Ault, B. S. *Rev. Chem. Intermed.* **1988**, *9*, 233.

(19) Ault, B. S.; Everhart, J. B. *J. Phys. Chem*. **1996**, *100*, 15726.

(20) Nelander, B. *J. Mol. Struc*. **1978**, *50*, 223.

(21) Bach, S. B. H.; Ault, B. S. *J. Phys. Chem*. **1984**, *88*, 3600.

(22) Barnes, A. J.; Hallam, H. E.; Howells, J. D. R.; Scrimshaw, G. F. *J. Chem. Soc., Faraday Trans. 2* **1973**, *69*, 738.

(23) Barnes, A. J. *J. Mol. Struct*. **1983**, *100*, 258.

(24) Bytheway, I.; Wong, M. W. *Chem. Phys. Lett*. **1998**, *282*, 219.